A Platinum Open Access Journal for Organic Chemistry

Paper

Free to Authors and Readers | DOAJ Seal | *Arkivoc* **2026** (2) 202612570

Ag and Au complexes of *N*-(2-pyridyl)thiourea: coordination behavior and antiproliferative properties

Rubén Gracia, Raquel P. Herrera,* and M. Concepción Gimeno*

Instituto de Síntesis Química y Catálisis Homogénea (ISQCH), CSIC-Universidad de Zaragoza, Pedro Cerbuna 12, 50009 Zaragoza, Spain

Email: raquelph@unizar.es, gimeno@unizar.es

Received 03-11-2026 **Accepted** 05-06-2026 **Published on line** 05-15-2026

Abstract

The coordination chemistry of *N*-(2-pyridyl)thiourea with Group 11 metals (Ag, Au) was explored with the aim of developing metal-based compounds with potential biological activity. The ligand preferentially binds soft metal centers through the thiourea sulfur atom, giving rise to well-defined coordination complexes. The cytotoxic properties of the free ligand and its metal derivatives were assessed *in vitro* against HeLa cervical cancer cells using the MTT assay. While the uncoordinated ligand exhibited no detectable cytotoxicity, several of its metal complexes showed pronounced antiproliferative effects, highlighting a synergistic contribution between the thiourea scaffold and the coordinated metal ions.

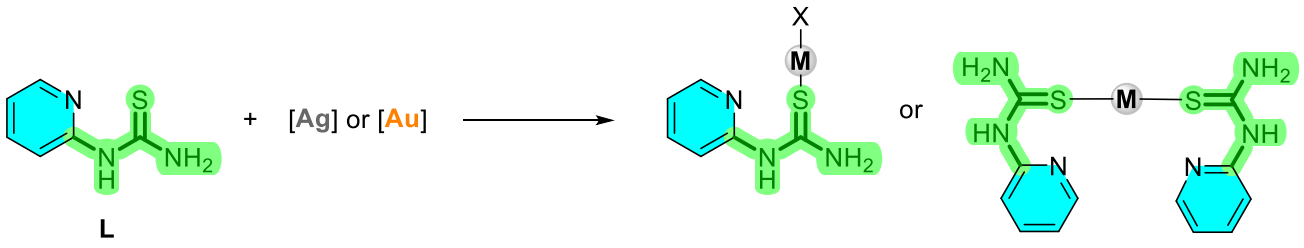

Keywords: Gold, silver, *N*-(2-pyridyl)thiourea, *in vitro*, cytotoxicity, HeLa.

Introduction

Thiourea derivatives constitute an important class of compounds in catalysis,[1-6] coordination[7] and medicinal chemistry[8-10] due to their structural versatility, rich electronic properties, and diverse coordination behavior. The presence of multiple heteroatoms, typically sulfur and nitrogen, together with extensive resonance stabilization, allows thioureas to act as flexible ligands, capable of binding metal centers in mono- or polydentate fashions, with acylthioureas being particularly effective ligands in metal complexes.[11-14] This adaptability has made thioureas valuable building blocks in a wide range of applications, including catalysis, materials science, and, increasingly, medicinal chemistry and agrochemistry.[15-18]

From a biological perspective, thiourea-based compounds have attracted considerable attention owing to their broad spectrum of pharmacological activities.[19] Numerous derivatives have been reported to exhibit antiproliferative, antimicrobial, antiviral, antiparasitic, and anti-inflammatory properties.[20-27] These activities are often attributed to the ability of thioureas to interact with biological targets through hydrogen bonding, metal chelation, and modulation of redox processes.[28]

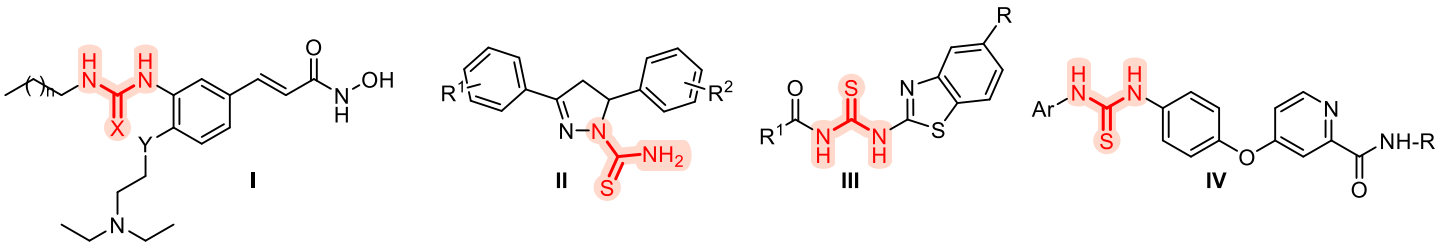

Figure 1. Thioureas with anticancer activity: **I**,[29] **II**,[20] **III**[30] and **IV**.[31]

Importantly, coordination of thiourea ligands to metal ions has been shown to significantly modify and, in many cases, enhance their biological behavior, suggesting a synergistic effect between the organic ligand framework and the metal center.

Group 11 metals (Cu, Ag, and Au) occupy a prominent position in bioinorganic and medicinal chemistry due to their unique electronic properties and well-documented biological activities.[32] Silver compounds are widely used as antimicrobial agents, owing to their ability to disrupt cellular membranes, bind to DNA, and interfere with essential enzymatic processes.[33-37] Copper, an essential trace element, plays a key role in redox biology and has been incorporated into a variety of metal-based therapeutic and diagnostic agents.[38-40]

Among group 11 metals, gold has emerged as particularly attractive for medicinal applications. Gold(I) complexes have a long history of clinical use in the treatment of rheumatoid arthritis, and, more recently, have gained attention for their potent anticancer, anti-inflammatory, and antimicrobial properties. Unlike classical platinum-based drugs, gold compounds often act through alternative mechanisms, such as inhibition of thiol- and selenol-containing enzymes, including thioredoxin reductase, a key regulator of cellular redox homeostasis and cancer cell proliferation. The strong affinity of gold(I) for soft-donor atoms, especially sulfur, makes thiourea ligands especially well-suited for stabilizing biologically relevant gold complexes.[41-43]

The combination of biologically active thiourea ligands with Group 11 metal centers represents a promising, yet still underexplored, strategy for the development of novel metal-based therapeutic agents.[44] Coordination to metal ions such as gold(I) and silver(I) can modulate the physicochemical and biological properties of thiourea derivatives, potentially leading to enhanced antiproliferative activity, and alternative mechanisms of action arising from synergistic interactions between the ligand framework and the metal

center. This approach has contributed to the growing interest in thiourea–metal complexes as candidates for anticancer applications. Nevertheless, the number of structurally characterized Ag(I) and Au(I) complexes incorporating thiourea ligands remains limited, and their coordination behavior and structure–activity relationships are not yet fully understood. In particular, *N*-(2-pyridyl)thiourea represents a promising ligand system due to the presence of both sulfur and nitrogen donor sites; however, its coordination chemistry with Ag(I) and Au(I), as well as the biological properties of the resulting complexes, have not been systematically investigated. The present study aims to address this gap by exploring the synthesis, structural characterization, and antiproliferative activity of Ag(I) and Au(I) complexes derived from *N*-(2-pyridyl)thiourea.

Results and Discussion

Synthesis of thiourea-metal complexes 1-6

Based on the considerations outlined above, the following section examines the metal complexes formed with ligand **L**, *N*-(2-pyridyl)thiourea, a thiourea-based ligand newly introduced into coordination chemistry and largely overlooked in previous studies.[45,46] This ligand was chosen due to its structural versatility and its potential to stabilize a wide range of metal centers through sulfur- and nitrogen-donor atoms. In this context, a series of reactions were carried out using silver and gold precursors, allowing exploration of the coordination sbehavior of **L** toward metals with different electronic and steric requirements. The results presented below provide insight into the reactivity patterns, structural features, and potential applications of the resulting complexes.

The reaction of ligand **L** with the silver complex [Ag(OTf)(PPh_3)] afforded complex **1** (Scheme 1). Although silver is known to form complexes with coordination numbers ranging from 2 to 4, in this case ligand **L** binds exclusively through the sulfur atom as depicted in Scheme 1. This coordination mode is consistent with the soft character of Ag(I) and the strong affinity of thiourea-type ligands for soft metal centers.

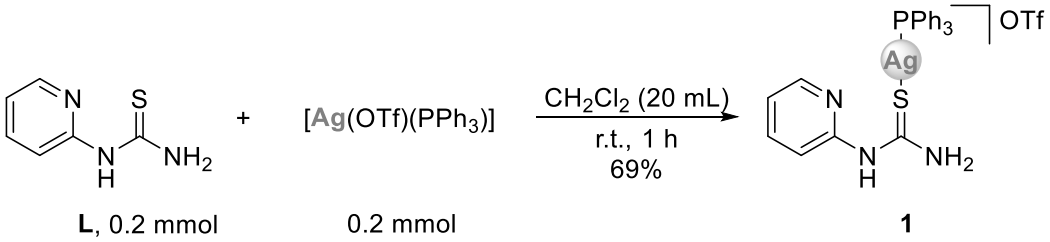

Scheme 1. Formation of the [AgL(PPh_3)]OTf complex **1**.

Coordination through the pyridine nitrogen atom is not supported. This assignment is based on the analysis of both IR and NMR spectra (see Supplementary Material file). In the infrared spectra, distinct shifts are observed in the bands corresponding to the pyridine-ring-stretching vibration, ν(C=C), and the C–S single-bond-stretching vibration, ν(C–S). Additionally, the ν(C=S) stretching band exhibits a slight shift, further indicating changes in the electronic environment upon coordination. The ^{1}H NMR spectrum provides additional evidence for this coordination mode. The signals assigned to the H-3 and H-2 protons of the pyridine ring show clear downfield shifts relative to the free ligand and display second-order splitting patterns. Moreover, a pronounced downfield shift is observed for one of the N–H proton resonances, consistent with coordination-induced electronic redistribution.

Complex **2** was synthesized by reacting one equivalent of ligand **L** with one equivalent of the silver precursor Ag(OTf). The resulting complex is proposed to involve coordination of the silver center through the sulfur atom of the thiourea moiety, as illustrated in Scheme 2.

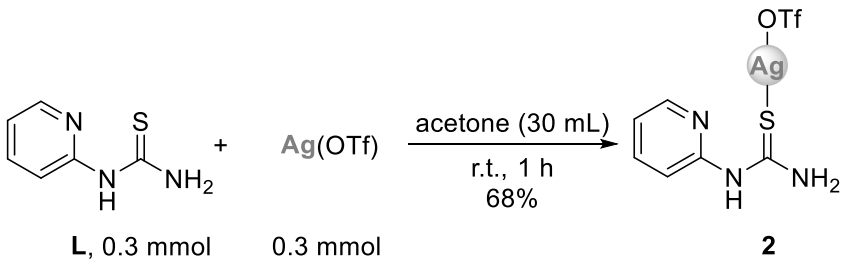

Scheme 2. Formation of the [AgL(OTf)] complex **2**.

In the infrared spectra, clear shifts are observed in the bands associated with the C–S stretching vibration and with the C=C stretching modes of the pyridine ring. These changes indicate a modification of the electronic environment of the ligand upon coordination. The ^{1}H NMR spectrum provides further support for the proposed coordination mode. The signals corresponding to H-2, H-3, and H-4 of the pyridine ring appear as a second-order system and undergo moderate shifts relative to the free ligand, consistent with the interaction of the metal center with the thiourea moiety. The resonances of the N–H protons also experience pronounced downfield shifts, reflecting changes in hydrogen bonding and electronic density upon complex formation. However, the pyridine proton H-1 does not exhibit a significant shift, suggesting that coordination through the pyridine nitrogen is unlikely in this complex.

The reaction between ligand **L** and Ag(OTf) was also carried out using a different molar ratio (2:1), employing two equivalents of the ligand per one equivalent of Ag(OTf). Under these conditions, the formation of complex **3** is proposed. As illustrated in Scheme 3, the silver center is expected to coordinate through the sulfur atom of each thiourea unit, giving rise to the corresponding bis-ligated complex.

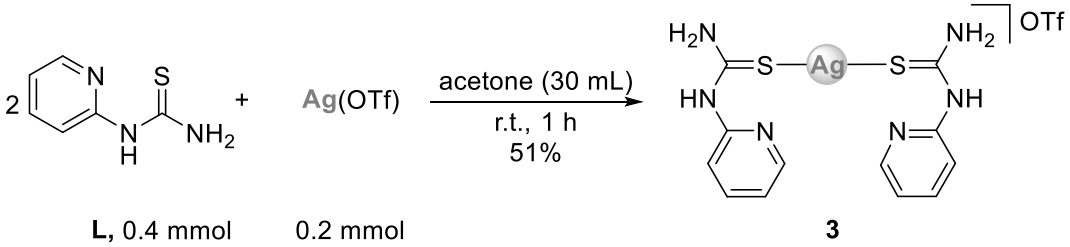

Scheme 3. Formation of the [AgL$_2$]OTf complex **3**.

To assess whether the proposed structure of the complex is correct, the infrared and ^{1}H NMR spectra of the isolated compound were analyzed. In the IR spectrum, the stretching band associated with the pyridine C=C double bond, ν(C=C), shows only minimal changes compared to the free ligand. In contrast, the stretching bands corresponding to the C–S and C=S bonds exhibit significant shifts, indicating a substantial modification of the thiourea environment upon coordination. The ^{1}H NMR spectrum provides additional insight. Only the signal corresponding to proton H-2 undergoes a pronounced shift, while the remaining pyridine protons show little variation relative to the free ligand. This behavior suggests that coordination does not occur through the

pyridine nitrogen atom. Instead, the observed spectral changes are consistent with coordination taking place through the sulfur atom of the thiourea moiety, as proposed.

In the following reaction, one equivalent of [Au(C_6F_5)(tht)] was reacted with one equivalent of ligand **L**. This procedure afforded complex **4**, whose formation is consistent with the reaction pathway illustrated in Scheme 4.

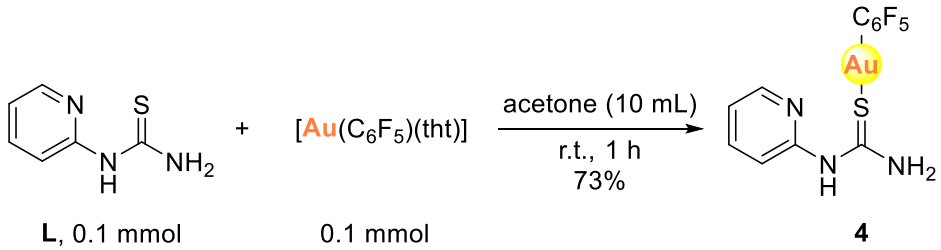

Scheme 4. Formation of the [Au(C_6F_5)L] complex **4**.

Confirmation of the proposed structure of complex **4** was pursued through analysis of the IR, ^{1}H NMR, and ^{19}F NMR spectra (see supporting information). In the infrared spectrum, the stretching bands associated with the C–S and C=S bonds exhibit noticeable shifts, confirming coordination of the gold center to the sulfur atom. In contrast, the pyridine C=C stretching region remains largely unchanged, indicating that the aromatic ring is not directly involved in the coordination process. The ^{1}H NMR spectrum of the metal complex shows clear shifts in the H-2 signal corresponding to the pyridine ring, as well as in the three N–H protons of the thiourea, reflecting the electronic perturbation induced by coordination. The ^{19}F NMR shows the typical pattern of pentafluorophenyl groups, with two multiplets for the *ortho* and *meta* fluorine, and a triplet for the *para* fluorine.

In the following reaction, one equivalent of [Au(OTf)(PPh_3)] was reacted with one equivalent of ligand **L**. The expected structure for complex **5** involves coordination of the gold center to the sulfur atom of the thiourea moiety, as illustrated in Scheme 5.

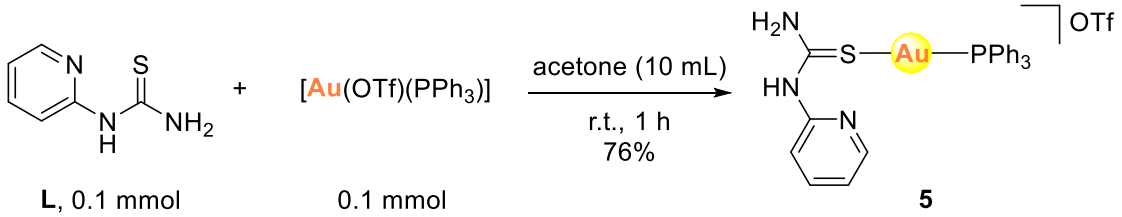

Scheme 5. Formation of the [AuL(PPh_3)]OTf complex **5**.

To confirm the proposed structure of complex **5**, the IR, ^{1}H NMR, and ^{31}P{^{1}H} NMR spectra were analyzed. In the infrared spectrum, only a slight shift is observed in the stretching band associated with the C–S bond, indicating a modest change in the thiourea environment upon coordination. In the ^{1}H NMR spectrum, the signals corresponding to the pyridine protons show minimal variation relative to the free ligand. In the ^{31}P NMR spectrum, a single resonance is observed at 38.5 ppm, corresponding to the phosphorus atom of triphenylphosphine. This chemical shift is characteristic of an S–Au–P coordination environment.

The structure of complex **5** was further confirmed by single-crystal X-ray diffraction. The molecular structure is shown in Figure 2a. The gold atom adopts a nearly linear coordination geometry, with a P1–Au1–

S1 angle of 176.04(5)°. The Au–P and Au–S bond distances are 2.2728(18) and 2.3237(18) Å, respectively, which lie within the typical range reported for gold–thiourea complexes.

A strong intramolecular interaction is observed between the pyridine nitrogen atom and one of the NH_2 protons, with an N···H distance of 1.816 Å, forming a six-membered ring that contributes to the stabilization of the molecular structure. In addition, several intermolecular short contacts are present between the oxygen atoms of the triflate group and the protons of the phenyl-substituted NH_2 groups, which can be classified as hydrogen-bonding interactions (Figure 2b).

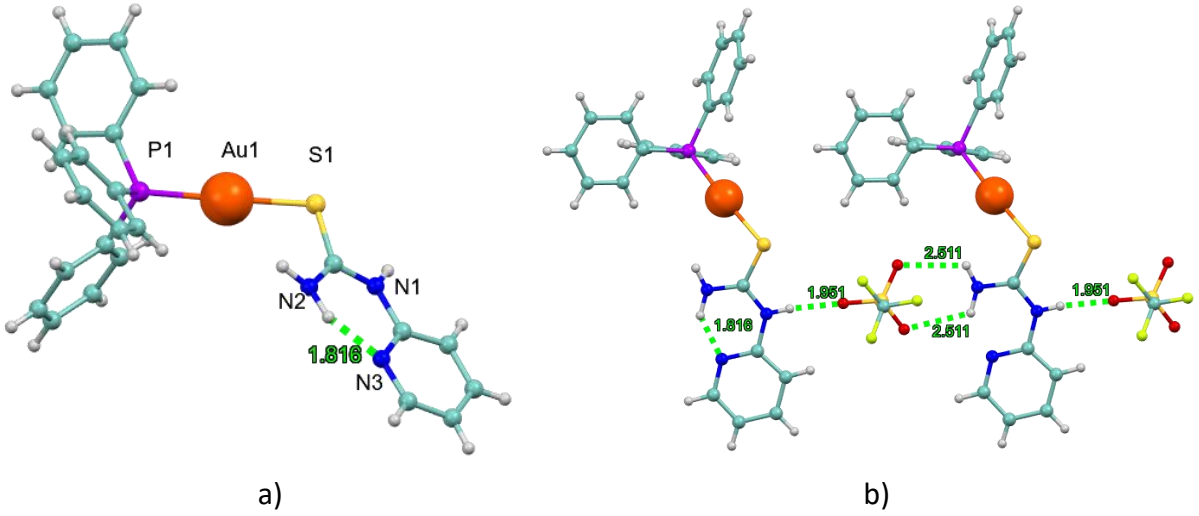

Figure 2. Molecular X-ray structure of complex **5** and intra- and intermolecular interactions.

Finally, one equivalent of the complex $[Au(tht)_2]OTf$ was reacted with two equivalents of ligand **L** to generate complex **6** (Scheme 6).

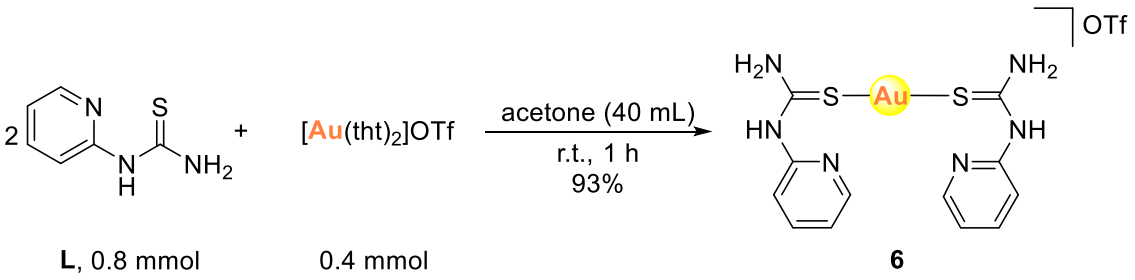

Scheme 6. Formation of the $[AuL_2]OTf$ complex **6**.

To confirm the proposed structure, the IR and ^1H NMR spectra were analyzed. In the infrared spectrum, a clear shift is observed in the band corresponding to the C–S stretching vibration, while the band associated with the pyridine C=C stretching mode remains essentially unchanged. This behavior suggests that coordination occurs exclusively through the sulfur atom. In the ^1H NMR spectrum, the signals corresponding to the ligand protons are shifted in comparison to those of the free ligand, consistent with coordination to the gold center.

Study of the cytotoxic activity of the thiourea-metal complexes 1-6 and thiourea ligand L

Based on our working hypothesis, coordination of thiourea ligands to Group 11 metal centers may generate compounds with enhanced antiproliferative activity, as both thiourea derivatives and gold(I) and silver(I) complexes are known to exhibit cytotoxic properties. To evaluate this possibility, the biological activities of ligand **L** and its corresponding metal complexes **1**–**6** were assessed using the MTT assay against HeLa human cervical cancer cells, a widely used model for investigating antiproliferative effects. The results are expressed as IC_{50} values (Table 1), defined as the concentration required to reduce cell viability by 50% relative to untreated control cells.

The free ligand **L** shows no detectable cytotoxic activity under the conditions examined, indicating that the thiourea scaffold alone is insufficient to induce significant antiproliferative effects. In contrast, coordination to Group 11 metal centers leads to a substantial enhancement of biological activity, highlighting the key role of the metal ion in modulating the pharmacological properties of the ligand. This behavior is consistent with the well-established ability of metal coordination to influence physicochemical properties such as stability, lipophilicity, and cellular uptake, thereby improving interactions with intracellular targets.

Table 1. IC_{50} values (μM) for complexes **1-6** and ligand **L** in HeLa cells after 24 h

Compound	IC_{50} (μM)
L	>100
[AgL(PPh_3)]OTf (**1**)	5.21 ± 0.66
[Ag(OTf)L] (**2**)	>100
[AgL_2]OTf (**3**)	6.08 ± 0.60
[Au(C_6F_5)L] (**4**)	17.94 ± 3.67
[AuL(PPh_3)]OTf (**5**)	7.70 ± 0.46
[AuL_2]OTf (**6**)	76.02 ± 1.83

A clear dependence of cytotoxic activity on both the metal center and the ligand environment is observed. Complexes **1** and **5** bearing triphenylphosphine as an auxiliary ligand display the highest activity, which may be attributed to the increased lipophilicity imparted by the phosphine group, facilitating membrane permeation and enhancing intracellular delivery. In addition, the strong σ-donor character of triphenylphosphine can modulate the electronic properties of the metal center, potentially favoring biologically relevant interactions.

Within the homoleptic bis(thiourea) series **3** and **6**, a marked difference between the silver(I) and gold(I) derivatives is observed, with the silver complex **3** exhibiting significantly higher activity than its gold analogue **6**. This difference may reflect variations in coordination stability, ligand exchange kinetics, and biological reactivity between the two metal ions. Silver(I) complexes are generally more labile than gold(I) complexes, which may promote interactions with intracellular biomolecules and contribute to enhanced cytotoxic effects.

The mixed-ligand gold complex **4** containing a pentafluorophenyl group shows intermediate activity, suggesting that the nature of the ancillary ligand also plays an important role in determining biological efficacy. Electronic and steric effects associated with the auxiliary ligand are likely to influence the stability, lipophilicity, and reactivity of the complex, thereby modulating its biological behavior. Unfortunately, silver complex **2** did not exhibit any biological activity, similar to the behavior of the free ligand. The marked differences in activity observed among complexes containing the same metal center (e.g., complexes **1**–**3** for

Ag and **4**–**6** for Au) indicate that the cytotoxic effects cannot be attributed to nonspecific metal residues, but rather to the specific coordination environment of each complex.

Overall, these results demonstrate that metal coordination is essential for inducing cytotoxic activity in this system and that both the identity of the metal center and the coordination environment strongly influence the antiproliferative properties. The enhanced activity observed for selected complexes highlights the potential of *N*-(2-pyridyl)thiourea as a promising ligand for the development of biologically active Group 11 metal complexes, and provides valuable insight into the structural factors governing their biological activity. Further studies will be necessary to elucidate their mechanisms of action and to evaluate their activity in additional biological models.

Conclusions

A series of mono- and bimetallic Group 11 metal complexes with *N*-(2-pyridyl)thiourea was successfully synthesized and characterized. The ligand displays selective coordination behavior, binding soft metal centers such as Ag(I) and Au(I), exclusively, through the thiourea sulfur atom. The pyridine nitrogen atom remains non-coordinating under the investigated conditions. Biological evaluation revealed that metal coordination significantly enhances antiproliferative activity compared to the free ligand, which is biologically inactive. Several complexes exhibit notable cytotoxic effects against HeLa cancer cells, with silver(I) and gold(I) complexes with the auxiliary PPh_3 ligand showing the most promising activity. These results highlight a synergistic effect between the thiourea ligand and the metal centers and support the potential of these compounds as candidates for further development in anticancer research.

Experimental Section

General. Commercially available compounds were used without further purification. NMR spectra were recorded on Bruker AV400 MHz spectrometer. ^{1}H NMR spectra were recorded at 400 MHz; ^{13}C{^{1}H}-APT NMR spectra were recorded at 100 MHz, ^{31}P{^{1}H} NMR was recorded at 162 MHz and ^{19}F at 376 MHz. Chemical shifts are described on the scale (δ ppm) relative to the residual peaks of acetone (2.05 ppm) and DMSO (2.50 ppm) for ^{1}H NMR and to the central line of $CD_3C(O)CD_3$ (29.8 ppm) and DMSO-d_6 (39.52 ppm) for ^{13}C{^{1}H}-APT NMR. ESI-MS spectra were obtained on Bruker MicroTof-Q mass spectrometer (Electrospray ESI). The ATR-FTIR spectra of solid samples were recorded on a PerkinElmer FT-IR spectrometer equipped with a universal ATR sampling accessory.

Crystals were mounted in inert oil on glass fibers and transferred to the cold gas stream of a Smart APEX CCD diffractometer equipped with a low-temperature (-173 °C) attachment. Data were collected using monochromated MoKα radiation (λ = 0.71073 Å). Data were collected using ω scans. Absorption corrections based on multiple scans were applied using SADABS.[47] The structure was solved by direct methods and refined on F2 using the program SHELXL-2016.[48] All nonhydrogen atoms were refined anisotropically. CCDC deposition numbers 2531829 (**5**), contain the supplementary crystallographic data. These data can be obtained free of charge from The Cambridge Crystallography Data Center.

Cytotoxicity assay. The MTT assay was used to determine cell viability as an indicator of cell sensitivity to the compounds. Exponentially growing cells were seeded at a density of approximately 15.000 cells per well (HeLa) in 96-well flat-bottom microplates (100 mL/well) and allowed to adhere for 24 h before addition of the compounds. The compounds were dissolved in DMSO and added to the cells at concentrations from 1 to 100 µM in quadruplicate. The DMSO concentration did not exceed 0.1% and appropriate controls with equivalent amounts of DMSO were performed. They were then left to incubate for 24 h at 37 °C. After this time, 10 µL of MTT (5 mg/mL) were added to each well and incubated again for 3 h at 37 °C. Finally, the culture medium was removed and 100 µL of DMSO per well was added to dissolve the formazan crystals. Optical density was measured at 490 nm using a 96-well multi-scanner auto-reader (ELISA). The IC_{50} is calculated by non-linear regression using Origin Pro software. Each compound was assayed a minimum of 3 times independently.

Characterization of ligand L. IR (cm^{-1}): ν(NH) = 3220; ν(NH) = 3057; ν(C=Car) = 1594, 1537, 1524, 766; ν(C=S) = 1233; (C-S) = 701, 678. ^{1}H NMR (ppm) (400 MHz, $CD_3C(O)CD_3$) *δ* 10.82 (br s, 1H, NH), 9.53 (br s, 1H, NH), 8.28 (ddd, 1H, *J* = 5.1, 1.9, 0.9 Hz, H(1)), 7.98 (br s, 1H, NH), 7.80 (ddd, *J* = 8.4, 7.3, 1.9 Hz, 1H, H(3)) 7.22 (dt, *J* = 8.4, 0.9 Hz, 1H, H(4)), 7.07 (ddd, *J* = 7.3, 5.1, 1.0 Hz, 1H, H(2)). ^{13}C{^{1}H}-APT NMR (ppm) (100 MHz, $CD_3C(O)CD_3$) *δ* 182.9 (s, 1C, C=S), 154.6 (s, 1C, C(5)), 147.1 (s, 1C, C(1)), 139.8 (s, 1C, C(3)), 118.9 (s, 1C, C(4)), 113.3 (s, 1C, C(2)). MS(ESI): *m/z* (%) = 154.0 for $C_6H_8N_3S$ $[M+H]^+$.

Synthesis of [AgL(PPh$_3$)]OTf 1. Ligand **L** (31 mg, 0.2 mmol) and [Ag(OTf)(PPh$_3$)] (103.3 mg, 0.2 mmol) were placed in a round-bottom flask and dissolved in 20 mL of dichloromethane. The reaction mixture was stirred for 1 h, during which no precipitation was observed. The solution was then concentrated to a minimum volume, and the addition of 10 mL of hexane induced the formation of a white solid. The product was finally collected by filtration and dried under vacuum. Yield: 69% (93 mg). IR (cm^{-1}): ν(NH) = 3254; ν(NH) = 3055; ν(C=Car) = 1603, 1528, 779; ν(C=S) = 1235; ν(C-S) = 779, 743. ^{1}H NMR (ppm) (400 MHz, $CD_3C(O)CD_3$) *δ* 11.56 (br s, 1H, NH), 10.43 (br s, 1H, NH), 9.17 (br s, 1H, NH), 8.28 (d, *J* = 5.0 Hz, 1H, H(1)), 7.89 (dt, *J* = 4.0, 8.0 Hz, 1H, H(3)), 7.61-7.38 (m, 15H, Ph), 7.36-7.18 (m, 2H, H(4), H(2)). ^{13}C{^{1}H}-APT NMR (ppm) (100 MHz, $CD_3C(O)CD_3$) *δ* 187.0 (s, 1C, C=S), 153.4 (s, 1C, C(5)), 147.3 (s, 1C, C(1)), 140.5 (s, 1C, C(3)), 134.6 (d, 6C, C_{ortho}-PPh_3, $^2J_{CP}$ = 16.2 Hz), 131.9 (d, 1C, C_{ipso}-PPh_3, $^2J_{CP}$ = 31.5 Hz), 131.8 (s, 3C, C_{para}-PPh_3), 130.1 (d, 6C, C_{meta}-PPh_3, $^2J_{CP}$ = 10.0 Hz), 121.1 (s, 1C, C(4)), 114.6 (s, 1C, C(2)). ^{31}P{^{1}H} NMR (ppm) (162 MHz, $CD_3C(O)CD_3$): 12.0 (br s, 1P, PPh_3). MS(ESI): *m/z* (%) = 523.0 for $C_{24}H_{22}AgN_3PS$ $[M\text{-}OTf]^+$.

Synthesis of [AgL(OTf)] 2. Ligand **L** (46 mg, 0.3 mmol) and Ag(OTf) (77.2 mg, 0.3 mmol) were placed in a round-bottom flask and dissolved in 30 mL of acetone. The reaction mixture was stirred for 1 h, during which no precipitation was observed. The solution was then concentrated to a minimum volume, and the addition of 10 mL of hexane induced the formation of a white solid. The product was finally collected by filtration and dried under vacuum. Yield: 68% (123 mg). IR (cm^{-1}): ν(NH) = 3278; ν(NH) = 3054; ν(C=Car) = 1642, 1610, 663; ν(C=S) = 1212; ν(C-S) = 776, 734. ^{1}H NMR (ppm) (400 MHz, $CD_3C(O)CD_3$) *δ* 11.8 (br s, 1H, NH), 10.5 (br s, 1H, NH), 9.35 (br s, 1H, NH), 8.38-8.36 (m, 1H, H(1)), 8.00-7.89 (m, 1H, H(3)), 7.37-7.22 (m, 2H, H(4),H(2)). ^{13}C{^{1}H}-APT NMR (ppm) (100 MHz, DMSO-d_6) *δ* 176.7 (s, 1C, C=S), 152.9 (s, 1C, C(5)), 146.3 (s, 1C, C(1)), 139.5 (s, 1C, C(3)), 119.5 (s, 1C, C(4)), 113.5 (s, 1C, C(2)). MS(ESI): *m/z* (%) = 260,0 for $C_6H_7AgN_3S$ $[M\text{-}OTf]^+$.

Synthesis of [AgL$_2$]OTf 3. Ligand **L** (61.3 mg, 0.4 mmol) and [AgOTf] (52.4 mg, 0.2 mmol) were placed in a round-bottom flask and dissolved in 30 mL of acetone. The reaction mixture was stirred for 1 h, during which no precipitation was observed. The solution was then concentrated to a minimum volume, and the addition of 10 mL of hexane induced the formation of a white solid. The product was finally collected by filtration and dried under vacuum. Yield: 51% (57 mg). IR (cm^{-1}): ν(NH) = 3255; ν(NH) = 3051; ν(C=Car) = 1603, 630; ν(C=S) = 1229; ν(C-S) = 774. ^{1}H NMR (ppm) (400 MHz, DMSO-d_6) δ 11.11(br s, 1H, NH), 11.07 (br s, 1H, NH), 9.60 (br s, 1H, NH), 8.31 (ddd, *J* = 5.1, 1.9, 0.8 Hz, 1H, H(1)), 7.87 (ddd, *J* = 8.4, 7.4, 1.9 Hz, 1H, H(3)), 7.26-7.12 (m, 2H,

H(4), H(2)). $^{13}C\{^{1}H\}$-APT NMR (ppm) (100 MHz, DMSO-d_6) δ 176.7 (s, 1C, C=S), 152.9 (s, 1C, C(5)), 146.3 (s, 1C, C(1)), 139.5 (s, 1C, C(3)), 119.5 (s, 1C, C(4)), 113.5 (s, 1C, C(2)). MS(ESI): *m/z* (%) = 414.0 for $C_{12}H_{14}AgN_6S_2$ [M-OTf] $^{+}$.

Synthesis of [Au(C_6F_5)L] 4. Ligand **L** (15.8 mg, 0.1 mmol) and [Au(C_6F_5)(tht)] (45.2 mg, 0.1 mmol) were placed in a round-bottom flask and dissolved in 10 mL of acetone. The reaction mixture was stirred for 1 h, during which no precipitation was observed. The solution was then concentrated to a minimum volume, and the addition of 10 mL of hexane induced the formation of a white solid. The product was finally collected by filtration and dried under vacuum. Yield: 73% (38 mg). IR (cm^{-1}): ν(NH) = 3407; ν(NH) = 3283; ν(C=Car) = 1602, 1585, 635; ν(C=S) = 1263; ν(C-F) = 1058; ν(C-S) = 766. ^{1}H NMR (ppm) (400 MHz, $CD_3C(O)CD_3$) δ 11.51 (br s, 1H, NH), 10.45 (br s, 1H, NH), 8.99 (br s, 1H, NH), 8.30 (ddd, *J* = 5.1, 1.9, 0.9 Hz, 1H, H(1)), 7.86 (ddd, *J* = 8.3, 7.4, 1.9 Hz, 1H, H(3)), 7.24 (dt, *J* = 8.3, 0.9 Hz, 1H, H(4)), 7.18 (ddd, *J* = 7.5, 5.1, 1.0 Hz, 1H, H(2)). $^{13}C\{^{1}H\}$-APT NMR (ppm) (100 MHz, $CD_3C(O)CD_3$) δ 177.5 (s, 1C, C=S), 153.7 (s, 1C, C(5)), 147.4 (s, 1C, C(1)), 140.7 (s,1C, C(3)), 121.2 (s, 1C, C(4)), 114.1 (s, 1C, C(2)). MS(ESI): *m/z* (%) = 517.0 for $C_{12}H_7AuF_5N_3S$ $[M]^{+}$.

Synthesis of [AuL(PPh_3)]OTf 5. Firstly, complex [Au(OTf)(PPh_3)] was generated *in situ* for use in the subsequent reaction. Silver triflate (Ag(OTf), 0.0051 g, 0.20 mmol) and [AuCl(PPh_3)] (0.0524 g, 0.20 mmol) were weighed and dissolved in 20 mL of dichloromethane. The mixture was stirred for 1 h, during which a white precipitate of AgCl is formed. The suspension was filtered to remove the solid, affording the desired gold complex in the filtration.

Ligand **L** (16.3 mg, 0.1 mmol) and [Au(OTf)(PPh_3)] (60.8 mg, 0.1 mmol) were placed in a round-bottom flask and dissolved in 10 mL of acetone. The reaction mixture was stirred for 1 h, during which no precipitation was observed. The solution was then concentrated to a minimum volume, and the addition of 10 mL of hexane induced the formation of a white solid. The product was finally collected by filtration and dried under vacuum. Yield: 76% (58 mg). IR (cm^{-1}): ν(NH) = 3236; ν(NH) = 3053; ν(C=Car) = 1597, 1524, 634; ν(C=S) = 1225; ν(C-S) = 774. 1H NMR (ppm) (400 MHz, $CD_3C(O)CD_3$) δ 11.28 (br s, 1H, NH), 10.14 (br s, 1H, NH), 8.71 (br s, 1H, NH), 8.33 (ddd, *J* = 5.1, 1.9, 0.9 Hz, 1H, H(1)), 7.89 (ddd, *J* = 8.4, 7.3, 1.9 Hz, 1H, H(3)), 7.83-7.37 (m, 7H, Ph) 7.26 (app. dt, *J* = 8.4, 0.9 Hz, 1H, H(4)), 7.14 (ddd, *J* = 7.4, 5.1, 1.0 Hz, 1H, H(2)). $^{13}C\{^{1}H\}$-APT NMR (ppm) (100 MHz, $CD_3C(O)CD_3$) δ 179.5 (s, 1C, C=S), 154.4 (s, 1C, C(5)), 147.2 (s, 1C, C(1)), 140.2 (s, 1C, C(3)), 135.1 (d, $^{2}J_{CP}$ = 14.0 Hz, 6C, C_{ortho}-Ph_3), 133.6 (s, 1C, C_{ipso}-PPh_3), 133.3 (d, $^{2}J_{CP}$ = 2.2 Hz 3C, C_{para}-PPh_3), 130.5 (d, $^{2}J_{CP}$ = 11.8 Hz, 6C, C_{meta}-PPh_3), 120.1 (s, 1C, C(4)), 114.1 (s, 1C, C(2)). $^{31}P\{^{1}H\}$ NMR (ppm) (162 MHz, $CD_3C(O)CD_3$): 38.7 (s, 1P, PPh_3). ^{19}F (376 MHz, $CD_3C(O)CD_3$): 117.5-117.6 (m, 2F), 163.5 (t, *J* = 18.8 Hz, 1F), 165.7-166.0 (m, 2F). MS(ESI): *m/z* (%) = 612.1 for $C_{24}H_{22}AuN_3PS$ $[M\text{-}OTf]^{+}$.

Synthesis of [AuL$_2$]OTf 6. Firstly, complex [Au(tht)$_2$]OTf was prepared as follows. [AuCl(tht)] (0.0392 g, 0.12 mmol) and [Ag(OTf)(tht)] (0.0422 g, 0.12 mmol) were weighed and dissolved in 30 mL of dichloromethane. The reaction mixture was stirred for 3 h, during which AgCl precipitated as a white solid. The suspension was then filtered to remove the insoluble AgCl, affording the desired gold complex in solution.

Ligand **L** (112.0 mg, 0.8 mmol) and [Au(tht)$_2$]OTf (302.0 mg, 0.4 mmol) were placed in a round-bottom flask and dissolved in 40 mL of acetone. The reaction mixture was stirred for 1 h, during which no precipitation was observed. The solution was then concentrated to a minimum volume, and the addition of 10 mL of hexane induced the formation of a white solid. The product was finally collected by filtration and dried under vacuum. Yield: 93% (243 mg). IR (cm^{-1}): ν(NH) = 3265; ν(NH) = 3192; ν(C_{sp2}-H) = 3059; ν(C=Car) = 1604, 1578, 621; ν(C=S) = 1235; ν(C-S) = 772. ^{1}H NMR (ppm) (400 MHz, $CD_3C(O)CD_3$) δ 11.73 (br s, 1H, NH), 10.75 (br s, 1H, NH), 9.44 (br s, 1H, NH), 8.41 (ddd, 1H, *J* = 5.1, 1.9, 0.9 Hz, H(1)), 7.98 (ddd, *J* = 8.4, 7.4, 1.9 Hz, 1H, H(3)), 7.38 (app. dt, *J* = 8.4, 0.9 Hz, 1H, H(4)), 7.31 (ddd, *J* = 7.3, 5.1, 1.0 Hz, 1H, H(2)). $^{13}C\{^{1}H\}$-APT NMR (ppm) (400 MHz,

$CD_3C(O)CD_3$) δ 175.3 (s, 1C, C=S), 153.8 (s, 1C, C(5)), 147.4 (s, 1C, C(1)), 140.7 (s, 1C, C(3)), 121.5 (s, 1C, C(4)), 115.0 (s, 1C, C(2)). MS(ESI): *m/z* (%) = 503.1 for $C_{12}H_{14}AuN_6S_2$ $[M\text{-}OTf]^+$.

Acknowledgements

The authors thank projects PID2022-136861NB-I00 and PID2023-147471NB-I00 funded by MICIU/AEI/ 10.13039/501100011033, and Gobierno de Aragon (Research Group E07_23R). Authors thank the Research Support Service of CEQMA (CSIC) and SAI (Universidad de Zaragoza).

Supplementary Material

Copies of ^1H, $^{13}C\{^1H\}$-APT, $^{31}P\{^1H\}$, ^{19}F NMR and IR spectra of all new compounds **1-6** are available in the Supplementary Material file associated with this paper.

References

1. Taylor, M. S.; Jacobsen, E. N. *Angew. Chem. Int. Ed.* **2006**, *45*, 1520. https://doi.org/10.1002/anie.200503132
2. Zhang, Z.; Schreiner, P. R. *Chem. Soc. Rev*. **2009**, *38*, 1187. https://doi.org/10.1039/B801793J
3. Narayanaperumal, S. Rivera, D. G.; Silva, R. C.; Paixão, M. W. *ChemCatChem* **2013**, *5*, 2756. https://doi.org/10.1002/cctc.201200936
4. Serdyuk, O. V.; Heckel, C. M.; Tsogoeva, S. B. *Org. Biomol. Chem*. **2013**, *11*, 7051. https://doi.org/10.1039/C3OB41403E
5. Zhang, Z.; Bao, Z.; Xing, H. *Org. Biomol. Chem*. **2014**, *12*, 3151. https://doi.org/10.1039/C4OB00306C
6. Rénio, M.; Ventura M. R. *Org. Biomol. Chem*. **2025**, *23*, 7521. https://doi.org/10.1039/D5OB00800J
7. Al-Halbosy, A. T. F.; Hamada, A. A.; Faihan, A. S.; Saleh, A. M.; Yousef, T. A.; Abou-Krisha, M. M.; Alhalafi, M. H.; Al-Janabi, A. S. M. *Inorganics* **2023**, *11*, 390. https://doi.org/10.3390/inorganics11100390
8. Ghosh, A. K.; Brindisi, M. *J. Med. Chem.* **2020**, *63*, 2751. https://doi.org/10.1021/acs.jmedchem.9b01541
9. Ronchetti, R.; Moroni, G.; Carotti, A.; Gioiello, A.; Camaioni, E. *RSC Med. Chem*. **2021**, *12*, 1046. https://doi.org/10.1039/D1MD00058F
10. Agili, F. A. *Chemistry* **2024**, *6*, 435. https://doi.org/10.3390/chemistry6030025
11. Koch, K. R. *Coord. Chem. Rev.* **2001**, *216*, 473. https://doi.org/10.1016/S0010-8545(01)00337-X
12. Zahra, U.; Saeed, A.; Fattah, T. A.; Flörke, U.; Erben, M. F. *RSC Adv.* **2022**, *12*, 12710. https://doi.org/10.1039/D2RA01781D

13. Ullah, S. A.; Saeed, A.; Azeem, M.; Haider, M. B.; Erben, M. F. *RSC Adv.* **2024**, *14*, 18011. https://doi.org/10.1039/D4RA02567A
14. Swaminathan, S.; Jerome, P.; Deepak, R. J.; Karvembu, R.; Oh, T. H. *Coord. Chem. Rev.* **2024**, *503*, 215620. https://doi.org/10.1016/j.ccr.2023.215620
15. Gimeno, M. C.; Herrera, R. P. *Cryst. Growth Des.* **2016**, *16*, 5091. https://doi.org/10.1021/acs.cgd.6b00683
16. Alegre-Requena, J. V.; Marqués-López, E.; Herrera, R. P.; Díaz, D. D. *CrystEngComm* **2016**, *18*, 3985. https://doi.org/10.1039/C5CE02526E
17. Gimeno, M. C.; Herrera, R. P. *Eur. J. Org. Chem.* **2020**, *2020*, 1057. https://doi.org/10.1002/ejoc.201901344
18. Yi, Q.-Q.; Sun, P.; Zhang, X.; Wang, H.; Wu, J. *J. Agric. Food Chem.* **2025**, *73*, 8756. https://doi.org/10.1021/acs.jafc.5c00430
19. Khan, S. A.; Singh, N.; Saleem, K. *Eur. J. Med. Chem.* **2008**, *43*, 2272. https://doi.org/10.1016/j.ejmech.2007.12.012
20. Yang, W.; Hu, Y.; Yang, Y.-S.; Zhang, F.; Zhang, Y.-B.; Wang, X.-L.; Tang, J.-F.; Zhong, W.-Q.; Zhu, H.-L. *Bioorg. Med. Chem.* **2013**, *21*, 1050. https://doi.org/10.1016/j.bmc.2013.01.013
21. Hu, H.; Lin, C.; Ao, M.; Ji, Y.; Tang, B.; Zhou, X.; Fang, M.; Zeng, J.; Wu, Z. *RSC Adv.* **2017**, *7*, 51640. https://doi.org/10.1039/C7RA08149A
22. Huang, R.-Z.; Zhang, B.; Huang, X.-C.; Liang, G.-B.; Qin, J.-M.; Pan, Y.-M.; Liao, Z.-X.; Wang, H.-S. *RSC Adv.* **2017**, *7*, 8866. https://doi.org/10.1039/C6RA25590F
23. dos Santos, L.; Lima, L. A.; Cechinel-Filho, V.; Corrêa, R.; de Campos Buzzi, F.; Nunes, R. J. *Bioorg. Med. Chem.* **2008**, *16*, 8526. https://doi.org/10.1016/j.bmc.2008.08.019
24. Chen, K.; Tan, Z.; He, M.; Li, J.; Tang, S.; Hewlett, I.; Yu, F.; Jin, Y.; Yan, M. *Chem. Biol. Drug Des.* **2010**, *76*, 25. https://doi.org/10.1111/j.1747-0285.2010.00981.x
25. Stefanska, J.; Szulczyk, D.; Koziol, A. E.; Miroslaw, B.; Kedzierska, E.; Fidecka, S.; Busonera, B.; Sanna, G.; Giliberti, G.; La Colla, P.; Struga, M. *Eur. J. Med. Chem.* **2012**, *55*, 205. https://doi.org/10.1016/j.ejmech.2012.07.020
26. Kocyigit-Kaymakcioglu, B.; Celen, A. O.; Tabanca, N.; Ali, A.; Khan, S. I.; Khan, I. A.; Wedge, D. E. *Molecules* **2013**, *18*, 3562. https://doi.org/10.3390/molecules18033562
27. Tong, J.-Y.; Sun, N.-B.; Wu, H.-K. *Asian J. Chem.* **2013**, 25, 5420. https://doi.org/10.14233/ajchem.2013.14444
28. Schmidtchen, F. P.; Berger, M. *Chem. Rev.* **1997**, *97*, 1609. https://doi.org/10.1021/cr9603845
29. Ning, C.; Bi, Y.; He, Y.; Huang, W. Y.; Liu, L.; Li, Y.; Zhang, S.; Liu, X.; Yu, N. *Bioorg. Med. Chem. Lett.* **2013**, *23*, 6432. https://doi.org/10.1016/j.bmcl.2013.09.051
30. Saeed, S.; Rashid, N.; Jones, P. G.; Ali, M.; Hussain, R. *Eur. J. Med. Chem.* **2010**, *45*, 1323. https://doi.org/10.1016/j.ejmech.2009.12.016
31. Yao, J.; Chen, J.; He, Z.; Sun, W.; Xu, W. *Bioorg. Med. Chem*. **2012**, *20*, 2923.

https://doi.org/10.1016/j.bmc.2012.03.018
32. Fernández-Moreira, V.; Herrera, R. P.; Gimeno, M. C. *Pure Appl. Chem.* **2019**, *91,* 247. https://doi.org/10.1515/pac-2018-0901
33. Banti, C. N.; Giannoulis, A. D.; Kourkoumelis, N.; Owczarzak, A. M.; Poyraz, M.; Kubicki, M.; Charalabopoulos, K.; Hadjikakou, S. K. *Metallomics* **2012**, *4*, 545. https://doi.org/10.1039/c2mt20039b
34. Banti, C. N.; Hadjikakou, S. K. *Metallomics* **2013**, *5*, 569. https://doi.org/10.1039/C3MT00046J
35. Medici, S.; Peana, M.; Nurchi, V. M.; Lachowicz, J. I.; Crisponi, G.; Zoroddu, M. A. *Coord. Chem. Rev.* **2015**, *284*, 329. https://doi.org/10.1016/j.ccr.2014.08.002
36. Fabbrini, M. G.; Cirri, D.; Pratesi, A.; Ciofi, L.; Marzo, T.; Guerri, A.; Nistri, S.; Dell'Accio, A.; Gamberi, T.; Severi, M.; Bencini, A.; Messori, L. *ChemMedChem* **2018**, *14*, 182. https://doi.org/10.1002/cmdc.201800672
37. Ota, A.; Tajima, M.; Mori, K.; Sugiyama, S.; Sato, V. H.; Sato, H. *Pharmacol. Rep.* **2021**, *73*, 847. https://doi.org/10.1007/s43440-021-00260-0
38. Festa, R. A.; Thiele, D. J. *Curr. Biol.* **2011**, *21*, pR877. https://doi.org/10.1016/j.cub.2011.09.040
39. Wang, P.; Yuan, Y.; Xu, K.; Zhong, H.; Yang, Y.; Jin, S.; Yang, K.; Qi, X. *Bioact. Mater.* **2020**, *6*, 916. https://doi.org/10.1016/j.bioactmat.2020.09.017
40. Krasnovskaya, O.; Naumov, A.; Guk, D.; Gorelkin, P.; Erofeev, A.; Beloglazkina, E.; Majouga, A. *Int. J. Mol. Sci.* **2020**, *21*, 3965. https://doi.org/10.3390/ijms21113965
41. Yan, K.; Lok, C.-N.; Bierla, K.; Che, C.-M. *Chem. Commun.* **2010**, *46*, 7691. https://doi.org/10.1039/C0CC01058H
42. Yu, B.; Liu, Y.; Peng, X.; Hua, S.; Zhou, G.; Yan, K.; Liu, Y. *Metallomics* **2020**, *12*, 104. https://doi.org/10.1039/C9MT00232D
43. Canudo-Barreras, G.; Ortego, L.; Izaga, A.; Marzo, I.; Herrera, R. P.; Gimeno, M. C. *Molecules* **2021**, *26*, 6891. https://doi.org/10.3390/molecules26226891
44. Dömling, A.; Klein, D.; Manoharan, S.; Mohr, F. *Chem. Lett.* **2025**, *54*, upaf116. https://doi.org/10.1093/chemle/upaf116
45. Satpathy, K. C.; Panda, A. K.; Mishra, R.; Mohapatra, A. *Syn. React. Inorg. Met.-Org. Chem.* **1989**, *19*, 23. https://doi.org/10.1080/00945718908048048
46. El-Ayaan, U. *J. Mol. Struct.* **2011**, *998*, 11. https://doi.org/10.1016/j.molstruc.2011.04.024
47. Sheldrick, G. M. SADABS, Program for adsorption correction, University of Göttingen, Göttingen, Germany, 1996.
48. Sheldrick, G. *Acta Crystallogr. Sec. A* **2015**, *71*, 3. https://doi.org/10.1107/S2053273314026370